J|A|C|S ARTICLES

Published on Web 12/24/2008

Activating Pd by Morphology Tailoring for Oxygen Reduction

Li Xiao,[†] Lin Zhuang,*[,†,‡,§] Yi Liu,[‡,§] Juntao Lu,[†] and Héctor D. Abruña*[,‡,§]

Department of Chemistry, Hubei Key Laboratory of Electrochemical Power Sources, Wuhan University, Wuhan 430072, China, Department of Chemistry and Chemical Biology, Baker Laboratory, Cornell Fuel Cell Institute (CFCI), Cornell University, Ithaca, New York 14853

Received August 12, 2008; E-mail: lzhuang@whu.edu.cn; hda1@cornell.edu

Abstract: Pd has been the focus of recent research for Pt-alternative catalysts for the oxygen reduction reaction (ORR). It has been found that upon appropriate modification of its electronic structure, the catalytic activity of Pd can become comparable to that of Pt. However, the structure−activity relationships of Pd catalysts have hitherto not been well studied or understood. In the present work, we report a new finding that there is a strong dependence of the activity of Pd toward the ORR on its morphology. By simply adjusting the precursor concentration in the electrochemical deposition of Pd, we are able to tailor the morphology of the deposited Pd from nanoparticles to nanorods. Surprisingly, the surface-specific activity of Pd nanorods (Pd-NRs) toward the ORR was found to be not only 10-fold higher than that of Pd nanoparticles (Pd-NPs), the conventional shape of electrocatalysts, but also comparable to that of Pt at operating potentials of fuel cell cathodes. The morphology−activity relationships of Pd-NRs were further studied through a combination of electrochemical experiments and density functional theory (DFT) calculations. As revealed by its characteristic profile for CO stripping, the morphology of Pd-NRs features the exposure of Pd(110) facets, which exhibit superior ORR activity. The underlying mechanism, indicated by DFT calculations, could be ascribed to the exceptionally weak interaction between an O adatom and a Pd(110) facet. This finding furthers our understanding of Pd catalysis and casts a new light on the relevant catalyst design criteria.

Introduction

Fuel cells, as a key technology for the future hydrogen-based economy, have seen great advances in recent decades.[1−6] Despite these efforts, there are still scientific and technological difficulties hampering the widespread commercialization of fuel cells. For instance, the sluggish kinetics of the oxygen reduction reaction (ORR) (cathode reaction) has been a major bottleneck in the performance of polymer electrolyte membrane fuel cells (PEMFCs), thus requiring intensive use of Pt catalysts. Such a heavy dependence on Pt, an expensive and scarce resource, would preclude the extensive application and widespread deployment of PEMFCs. To address this issue, approaches for maximizing the Pt utilization and searching for Pt-alternative catalysts must be pursued. On the one hand, great attention has been paid to increasing the dispersion and stability of Pt nanoparticles,[7−13] as well as to developing advanced Pt catalysts with specific shapes,[14−26] bimetallic/intermetallic compositions,[27−34] and core−shell structures.[35−41] On the other hand,

[†] Wuhan University.
[‡] Department of Chemistry and Chemical Biology, Cornell University.
[§] Cornell Fuel Cell Institute (CFCI), Cornell University.

(1) Borup, R.; et al. *Chem. Rev.* **2007**, *107*, 3904.
(2) Bashyam, R.; Zelenay, P. *Nature* **2006**, *443*, 63.
(3) Jacobson, M. Z.; Colella, W. G.; Golden, D. M. *Science* **2005**, *308*, 1901.
(4) Wang, C. Y. *Chem. Rev.* **2004**, *104*, 4727.
(5) Schultz, M. G.; Diehl, T.; Brasseur, G. P.; Zittel, W. *Science* **2003**, *302*, 624.
(6) Steele, B. C. H.; Heinzel, A. H. *Nature* **2001**, *414*, 345.
(7) Warren, S. C.; Messina, L. C.; Slaughter, L. S.; Kamperman, M.; Zhou, Q.; Gruner, S. M.; DiSalvo, F. J.; Wiesner, U. *Science* **2008**, *320*, 1748.
(8) Zhang, J.; Sasaki, K.; Sutter, E.; Adzic, R. R. *Science* **2007**, *315*, 220.
(9) Sun, Y.; Zhuang, L.; Lu, J.; Hong, X.; Liu, P. *J. Am. Chem. Soc.* **2007**, *129*, 15465.
(10) Wang, L.-L.; Johnson, D. D. *J. Am. Chem. Soc.* **2007**, *129*, 3658.
(11) Kim, Y.-T.; Ohshima, K.; Higashimine, K.; Uruga, T.; Takata, M.; Suematsu, H.; Mitani, T. *Angew. Chem., Int. Ed.* **2006**, *45*, 407.
(12) Ye, H.; Crooks, R. M. *J. Am. Chem. Soc.* **2005**, *127*, 4930.
(13) Joo, S. H.; Choi, S. J.; Oh, I.; Kwak, J.; Liu, Z.; Terasaki, O.; Ryoo, R. *Nature* **2001**, *412*, 169.
(14) Yamauchi, Y.; Sugiyama, A.; Morimoto, R.; Takai, A.; Kuroda, K. *Angew. Chem., Int. Ed.* **2008**, *47*, 5371.
(15) Wang, C.; Daimon, H.; Onodera, T.; Koda, T.; Sun, S. *Angew. Chem., Int. Ed.* **2008**, *47*, 3588.
(16) Fan, F.-R.; Liu, D.-Y.; Wu, Y.-F.; Duan, S.; Xie, Z.-X.; Jiang, Z.-Y.; Tian, Z.-Q. *J. Am. Chem. Soc.* **2008**, *130*, 6949.
(17) Mahmoud, M. A.; Tabor, C. E.; EI-Sayed, M. A.; Ding, Y.; Wang, Z. L. *J. Am. Chem. Soc.* **2008**, *130*, 4590.
(18) Tian, N.; Zhou, Z.-Y.; Sun, S.-G.; Ding, Y.; Wang, Z. L. *Science* **2007**, *316*, 732.
(19) Cui, G.; Zhi, L.; Thomas, A.; Kolb, U.; Lieberwirth, I.; Müllen, K. *Angew. Chem., Int. Ed.* **2007**, *46*, 3464.
(20) Chen, Z.; Waje, M.; Li, W.; Yan, Y. *Angew. Chem., Int. Ed.* **2007**, *46*, 4060.
(21) Wang, C.; Daimon, H.; Lee, Y.; Kim, J.; Sun, S. *J. Am. Chem. Soc.* **2007**, *129*, 6974.
(22) Lee, H. L.; Habas, S. E.; Kweskin, S.; Butcher, D.; Somorjai, G. A.; Yang, P. *Angew. Chem., Int. Ed.* **2006**, *45*, 7824.
(23) El-Deab, M. S.; Ohsaka, T. *Angew. Chem., Int. Ed.* **2006**, *45*, 5963.
(24) Ding, Y.; Mathur, A.; Chen, M.; Erlebacher, J. *Angew. Chem., Int. Ed.* **2005**, *44*, 4002.
(25) Narayanan, R.; EI-Sayed, M. A. *Nano Lett.* **2004**, *4*, 1343.
(26) Ahmadi, T. S.; Wang, Z. L.; Green, T. C.; Henglein, A.; EI-Sayed, M. A. *Science* **1996**, *272*, 1924.
(27) Abe, H.; Matsumoto, F.; Alden, L. R.; Warren, S. C.; Abruña, H. D.; DiSalvo, F. J. *J. Am. Chem. Soc.* **2008**, *130*, 5452.
(28) Stamenkovic, V. R.; Fowler, B.; Mun, B. S.; Wang, G.; Ross, P. N.; Lucas, C. A.; Marković, N. M. *Science* **2007**, *315*, 493.

 10.1021/ja8063765 CCC: $40.75

tremendous efforts have been devoted to the search for non-Pt catalysts[2,42−104] with more recent efforts being focused on Pd.[53−104]

While Pd is the most Pt-like metal and a relatively abundant resource, its catalytic activity toward the ORR appears to be much lower than that of Pt. Recent investigations have found that alloying Pd with some transition metals, such as Co,[53−75] Fe,[76−78] etc., is an effective way of improving the catalytic activity of Pd. In fact, some of these Pd alloys showed activity and stability comparable to those of Pt catalysts.[68,69,78] Albeit promising and stimulating, the underlying science of such promotion effects remains an unsolved subject of great interest for fuel cell development. Some researchers postulated that the alloying component could play a synergistic role in the surface of Pd,[70,71] which alters the thermodynamics and/or the kinetics

(29) Stamenkovic, V. R.; Mun, B. S.; Arenz, M.; Mayrhofer, K. J. J.; Lucas, C. A.; Wang, G.; Ross, P. N.; Markovic, N. M. *Nat. Mater.* **2007**, *6*, 241.
(30) Maksimuk, S.; Yang, S.; Peng, Z.; Yang, H. *J. Am. Chem. Soc.* **2007**, *129*, 8684.
(31) Stamenkovic, V.; Mum, B. S.; Mayrhofer, K. J. J.; Ross, P. N.; Markovic, N. M.; Rossmeisl, J.; Greeley, J.; Nørskov, J. K. *Angew. Chem., Int. Ed.* **2006**, *45*, 2897.
(32) Greeley, J.; Mavrikakis, M. *Nat. Mater.* **2004**, *3*, 810.
(33) Xu, Y.; Ruban, A. V.; Mavrikakis, M. *J. Am. Chem. Soc.* **2004**, *126*, 4717.
(34) Casado-Rivera, E.; Volpe, D. J.; Alden, L.; Lind, C.; Downie, C.; Vázquez-Alvarez, T.; Angelo, A. C. D.; DiSalvo, F. J.; Abruña, H. D. *J. Am. Chem. Soc.* **2004**, *126*, 4043.
(35) Alayoglu, S.; Nilekar, A. U.; Mavrikakis, M.; Eichhorn, B. *Nat. Mater.* **2008**, *7*, 333.
(36) Srivastava, R.; Mani, P.; Hahn, N.; Strasser, P. *Angew. Chem., Int. Ed.* **2007**, *46*, 8988.
(37) Koh, S.; Strasser, P. *J. Am. Chem. Soc.* **2007**, *129*, 12624.
(38) Zhao, D.; Xu, B. Q. *Angew. Chem., Int. Ed.* **2006**, *45*, 4955.
(39) Stamenkovic, V. R.; Mum, B. S.; Mayrhofer, K. J. J.; Ross, P. N.; Markovic, N. M. *J. Am. Chem. Soc.* **2006**, *128*, 8813.
(40) Zhang, J.; Vukmirovic, M. B.; Sasaki, K.; Nilekar, A. U.; Mavrikakis, M.; Adzic, R. R. *J. Am. Chem. Soc.* **2005**, *127*, 12480.
(41) Zhang, J.; Vukmirovic, M. B.; Xu, Y.; Mavrikakis, M.; Adzic, R. R. *Angew. Chem., Int. Ed.* **2005**, *44*, 2132.
(42) Winther-Jensen, B.; Winther-Jensen, O.; Forsyth, M.; MacFarlane, D. R. *Science* **2008**, *321*, 671.
(43) Zehl, G.; Schmithals, G; Hoell, A.; Haas, S.; Hartnig, C.; Dorbandt, I.; Bogdanoff, P.; Fiechter, S. *Angew. Chem., Int. Ed.* **2007**, *46*, 7311.
(44) Givaja, G.; Volpe, M.; Edwards, M. A.; Blake, A. J.; Wilson, C.; Schröder, M.; Love, J. B. *Angew. Chem., Int. Ed.* **2007**, *46*, 584.
(45) Babu, P. K.; Lewera, A.; Chung, J. H.; Hunger, R.; Jaegermann, W.; Alonso-Vante, N.; Wieckowski, A.; Oldfield, E. *J. Am. Chem. Soc.* **2007**, *129*, 15140.
(46) Weng, Y. C.; Fan, F.-R. F.; Bard, A. J. *J. Am. Chem. Soc.* **2005**, *127*, 17576.
(47) Kadish, K. M.; Frémond, L.; Ou, Z.; Shao, J.; Shi, C.; Anson, F. C.; Burdet, F.; Gros, C. P.; Barbe, J.-M.; Guilard, R. *J. Am. Chem. Soc.* **2005**, *127*, 5625.
(48) Li, X.; Gewirth, A. A. *J. Am. Chem. Soc.* **2005**, *127*, 5252.
(49) Fukuzumi, S.; Okamoto, K.; Tokuda, Y.; Gros, C. P.; Guilard, R. *J. Am. Chem. Soc.* **2004**, *126*, 17059.
(50) Fukuzumi, S.; Okamoto, K.; Gros, C. P.; Guilard, R. *J. Am. Chem. Soc.* **2004**, *126*, 10441.
(51) Chang, C. J.; Loh, Z.-H.; Shi, C.; Anson, F. C.; Nocera, D. G. *J. Am. Chem. Soc.* **2004**, *126*, 10013.
(52) Cole, A. P.; Root, D. E.; Mukherjee, P.; Solomon, E. I.; Stack, T. D. P. *Science* **1996**, *273*, 1848.
(53) Liu, H.; Manthiram, A. *Electrochem. Commum.* **2008**, *10*, 740.
(54) Lin, C.-L.; Sánchez-Sánchez, C. M.; Bard, A. *J. Electrochem. Solid-State Lett.* **2008**, *11*, B136.
(55) Suo, Y.; Zhuang, L.; Lu, J. *Angew. Chem., Int. Ed.* **2007**, *46*, 2862.
(56) Shao, M.; Sasaki, K; Marinkovic, N. S.; Zhang, L.; Adzic, R. R. *Electrochem. Commun.* **2007**, *9*, 2848.
(57) Tarasevich, M. R.; Bogdanovskaya, V. A.; Kuznetsova, L. N.; Modestov, A. D.; Efremov, B. N.; Chalykh, A. E.; Chirkov, Y. G.; Kapustina, N. A.; Ehrenburg, M. R. *J. Appl. Electrochem.* **2007**, *37*, 1503.
(58) Noto, V. D.; Negro, E.; Lavina, S.; Gross, S.; Pace, G. *Electrochim. Acta* **2007**, *53*, 1604.
(59) Zhang, L.; Lee, K.; Zhang, J. *Electrochim. Acta* **2007**, *52*, 7964.
(60) Mustain, W. E.; Kepler, K.; Prakash, J. *Electrochim. Acta* **2007**, *52*, 2102.
(61) Zhang, L.; Lee, K.; Zhang, J. *Electrochim. Acta* **2007**, *52*, 3088.
(62) Mustain, W. E.; Prakash, J. *J. Power Sources* **2007**, *170*, 28.
(63) Wang, W.; Zheng, D.; Du, C.; Zou, Z.; Zhang, X.; Xia, B.; Yang, H.; Akins, D. L. *J. Power Sources* **2007**, *167*, 243.
(64) Mathiyarasu, J.; Phani, K. L. N. *J. Electrochem. Soc.* **2007**, *154*, B1100.
(65) Gu, Z.; Balbuena, P. B. *J. Phys. Chem. A* **2006**, *110*, 9783.
(66) Lamas, E. J.; Balbuena, P. B. *J. Chem. Theory Comput.* **2006**, *2*, 1388.
(67) Lee, K.; Savadogo, O.; Ishihara, A.; Mitsushima, S.; Kamiya, N.; Ota, K. *J. Electrochem. Soc.* **2006**, *153*, A20.
(68) Raghuveer, V.; Ferreira, P. J.; Manthiram, A. *Electrochem. Commun.* **2006**, *8*, 807.
(69) Fernández, J. L.; Raghuveer, V.; Manthiram, A.; Bard, A. J. *J. Am. Chem. Soc.* **2005**, *127*, 13100.
(70) Fernández, J. L.; Walsh, D. A.; Bard, A. J. *J. Am. Chem. Soc.* **2005**, *127*, 357.
(71) Wang, Y.; Balbuena, P. B. *J. Phys. Chem. B* **2005**, *109*, 18902.
(72) Raghuveer, V.; Manthiram, A.; Bard, A. J. *J. Phys. Chem. B* **2005**, *109*, 22909.
(73) Tarasevich, M. R.; Chalykh, A. E.; Bogdanovskaya, V. A.; Kuznetsova, L. N.; Kapustina, N. A.; Efremov, B. N.; Ehrenburg, M. R.; Reznikova, L. A. *Electrochim. Acta* **2005**, *51*, 4455.
(74) Savadogo, O.; Lee, K.; Mitsushima, S.; Kamiya, N.; Ota, K. I. *J. New Mater. Electrochem. Syst.* **2004**, *2*, 77.
(75) Savadogo, O.; Lee, K.; Oishi, K.; Mitsushima, S.; Kamiya, N.; Ota, K.-I. *Electrochem. Commun.* **2004**, *6*, 105.
(76) Wang, R.; Liao, S.; Fu, Z.; Ji, S. *Electrochem. Commun.* **2008**, *10*, 523.
(77) Shao, M.; Liu, P.; Zhang, J.; Adzic, R. *J. Phys. Chem. B* **2007**, *111*, 6772.
(78) Shao, M.-H.; Sasaki, K.; Adzic, R. R. *J. Am. Chem. Soc.* **2006**, *128*, 3526.
(79) Okamoto, Y. *J. Phys. Chem. C* **2008**, *112*, 5888.
(80) Sarkar, A.; Murugan, A. V.; Manthiram, A. *J. Phys. Chem. C* **2008**, *112*, 12037.
(81) Shen, Y.; Träuble, M.; Wittstock, G. *Phys. Chem. Chem. Phys.* **2008**, *10*, 3635.
(82) Yang, J.; Lee, J. Y.; Zhang, Q.; Zhou, W.; Liu, Z. *J. Electrochem. Soc.* **2008**, *155*, B776.
(83) Wang, X.; Kariuki, N.; Vaughey, J. T.; Goodpaster, J.; Kumar, R.; Myers, D. J. *J. Electrochem. Soc.* **2008**, *155*, B602.
(84) Cheng, F.; Wang, H.; Sun, Z.; Ning, M.; Cai, Z.; Zhang, M. *Electrochem. Commun.* **2008**, *10*, 798.
(85) Xu, C.; Wang, H.; Shen, P. K.; Jiang, S. P. *Adv. Mater.* **2007**, *19*, 4256.
(86) Ye, H.; Crooks, R. M. *J. Am. Chem. Soc.* **2007**, *129*, 3627.
(87) Li, H.; Sun, G.; Li, N.; Sun, S.; Su, D.; Xin, Q. *J. Phys. Chem. C* **2007**, *111*, 5605.
(88) Nilekar, A. U.; Xu, Y.; Zhang, J.; Vukmirovic, M. B.; Sasaki, K.; Adzic, R. R.; Mavrikakis, M. *Top. Catal.* **2007**, *46*, 276.
(89) Spendelow, J. S.; Wieckowski, A. *Phys. Chem. Chem. Phys.* **2007**, *9*, 2654.
(90) Vukmirovic, M. B.; Zhang, J.; Sasaki, K.; Nilekar, A. U.; Uribe, F.; Mavrikakis, M.; Adzic, R. R. *Electrochim. Acta* **2007**, *52*, 2257.
(91) Zheng, J.-S.; Zhang, X.-S.; Li, P.; Zhu, J.; Zhou, X.-G.; Yuan, W.-K. *Electrchem. Commun.* **2007**, *9*, 895.
(92) Salvador-Pascual, J. J.; Citalán-Cigarroa, S.; Solorza-Feria, O. *J. Power Sources* **2007**, *172*, 229.
(93) Nie, M.; Shen, P. K.; Wei, Z. D. *J. Power Sources* **2007**, *167*, 69.
(94) Walsh, D. A.; Fernández, J. L.; Bard, A. J. *J. Electrochem. Soc.* **2006**, *153*, E99.
(95) Shao, M. H.; Huang, T.; Liu, P.; Zhang, J.; Sasaki, K.; Vukmirovic, M. B.; Adzic, R. R. *Langmuir* **2006**, *22*, 10409.
(96) Yang, C.-C.; Kumar, A. S.; Zen, J.-M. *Electroanalysis* **2006**, *18*, 64.
(97) Lee, C.-L.; Huang, Y.-C.; Kuo, L.-C.; Oung, J.-C; Wu, F.-C. *Nanotechnology* **2006**, *17*, 2390.
(98) Lin, Y.; Cui, X.; Ye, X. *Electrochem. Commun.* **2005**, *7*, 267.
(99) Li, H.; Xin, Q.; Li, W.; Zhou, Z.; Jiang, L.; Yang, S.; Sun, G. *Chem. Commun.* **2004**, 2776.
(100) Arenz, M.; Schmidt, T. J.; Wandelt, K.; Ross, P. N.; Markovic, N. M. *J. Phys. Chem. B* **2003**, *107*, 9813.
(101) Giacomini, M. T.; Balasubramanian, M.; Khalid, S.; McBreen, J.; Ticianelli, E. A. *J. Electrochem. Soc.* **2003**, *150*, A588.
(102) Shen, Y.; Bi, L.; Liu, B.; Dong, S. *New J. Chem.* **2003**, *27*, 938.
(103) Naohara, H.; Ye, S.; Uosaki, K. *Electrochim. Acta* **2000**, *45*, 3305.
(104) Climent, V.; Marković, N. M.; Ross, P. N. *J. Phys. Chem. B* **2000**, *104*, 3116.

of the elementary steps of the ORR. Others emphasized the modulation effects in the electronic structure of Pd,[55,67,77] which, to a great extent, influences the surface reactivity. In previous work,[55] we found that the contraction in the Pd lattice, caused by the incorporation of foreign atoms of smaller diameter and leading to a decrease in the bonding strength of O_{ads}, could be an important reason for the improvement in the catalytic activity toward the ORR.

In fact, the number of studies of Pd-catalyzed ORR is well below that of the extensively studied Pt. Most investigations of Pd have been conducted using nanosized materials, which, albeit closely related to applications, bring complicated effects, such as uncertainty of surface structure and dependence on preparation methods, particle size and distribution, in addition to the electronic effects one would anticipate. In an effort to capture the catalytic essence, we carried out our studies of the Pd-catalyzed ORR on the basis of extended surfaces. Specifically, the intent was to electrochemically deposit Pd and Pd alloys onto a rotating disk electrode (RDE) and then study the ORR electrocatalysis using the methods that have been widely used for the Pt-catalyzed ORR.

In this work, we employed an RDE with an interchangeable Au substrate, which could be removed after Pd deposition for characterization using X-ray diffraction (XRD) and scanning electron microscopy (SEM). This enabled us to relate the electrochemical characteristics of the Pd electrode with structural features including surface morphology. The obvious advantage of this method was made evident by the main finding reported in the present paper: an unexpectedly strong dependence of the activity of Pd toward the ORR on its morphology. We have found that the morphology of Pd electrodes can be tailored by simply adjusting the precursor concentration and two typical morphologies, nanoparticles and nanorods, could be controllably, deliberately, and reproducibly obtained, which exhibited distinct activities toward the ORR. We also discuss the possible origin of the high activity of Pd nanorods toward the ORR based on a combination of electrochemical experiments and density functional theory (DFT) calculations.

Experimental and Computational Section

Electrochemical Deposition. Electrochemical deposition of Pd onto a Au RDE (5 mm in diameter) (Pine Research Instruments) was performed at a rotation rate of 1600 rpm in a deaerated 0.1 M NaCl solution containing $PdCl_2$ (Aldrich), the concentration of which was varied as described below. A Pd sheet was used as the counter electrode, and a Ag/AgCl (0.1 M NaCl) served as the reference electrode. The deposition potential was fixed at −0.2 V. The potentiostat was a CHI660 electrochemical station. The RDE system consisted of a PINE rotator and an interchangeable electrode (E6 Series). All chemicals were of at least analytical grade, and solutions were prepared using deionized water (Millipore, 18 MΩ·cm). All experiments were conducted at room temperature.

Cyclic Voltammetry (CV). The as-prepared Pd electrode was cleaned repeatedly via rotating in deionized water prior to the following tests. Cyclic voltammetry was carried out in deaerated 0.1 M $HClO_4$ (Aldrich, 99.999%) solution. A sheet of graphite paper (Toray), rather than metals such as Pt, was used as the counter electrode so as to exclude any possibility of metal contamination of the Pd electrode during experiments. The reference electrode was a reversible hydrogen electrode (RHE) in the same solution.

CO Stripping. CO stripping experiments were conducted under the same conditions as CV measurements except that the Pd electrode surface was preadsorbed with CO. The CO adsorption procedure was accomplished by polarizing the electrode at +0.4 V and bubbling the solution with CO for 10 min and subsequently with Ar for another 10 min.

ORR Evaluation. ORR evaluation was carried out under the same conditions as CV measurements in an O_2 saturated solution. The rotation rate was 900 rpm, and the ORR curves were recorded by scanning the potential from +0.4 V to +1.0 V at 10 mV/s.

Grazing-Incidence X-ray Diffraction (GID) Measurements. GID experiments were performed on a homemade six-circle *kappa* diffractometer[105] at the G2 Station of the Cornell High Energy Synchrotron Source (CHESS). The X-ray beam energy was 9.4 keV. The beam size was 2 mm horizontal by 200 μm vertical. The flux at the center of rotation was $\sim 10^{11}$ photons/sec·mm^2. The scanning range of the 2θ angle was from 30° to 40°, covering the Pd(111) and Pd(200) diffraction peaks.

SEM Observation. The Pd-deposited Au disk was taken out from the RDE and subjected to SEM observations using a field emission scanning electron microscope (KECK FE-SEM LEO-1550). To better image surface details, a low accelerating voltage of 3 kV was applied.

Transmission Electron Microscopy (TEM) Observation. For TEM observation, the Au RDE surface was covered with carbon powder (Vulcan XC-72, Carbot) prior to Pd deposition. The thus-obtained carbon-supported Pd deposits were peeled off from the Au substrate via sonication and dispersed in ethanol. TEM observations were conducted using a 200 kV field emission transmission electron microscope with a monochromator (FEI Tecnai F20).

DFT Calculations. DFT calculations were performed using the DACAPO code[106] with calculating parameters chosen for both the convergence in energy and relatively less computational effort. A 2×2 unit cell was used to construct a four-layer metal slab, corresponding to a 1/4 ML coverage of the adsorbate, and repeated in super cell geometry with successive slabs separated by a vacuum region equivalent to 6 metal layers. Adsorption was allowed on only one of the two exposed surfaces. The adsorbate layer and the top two layers of the slab were allowed to relax. The surface Brillouin zone was sampled at 6×6 special Chadi−Cohen *k*-points. The Kohn−Sham one-electron valence states were expanded in a basis of plane waves with kinetic energies up to 25 Ry, and ionic cores were described by ultrasoft pseudopotentials. The exchange-correlation potential and energy were described self-consistently using the GGA-PW91 functional.

Results and Discussion

Pd Nanorods (Pd-NRs) and Pd Nanoparticles (Pd-NPs). The electrochemical deposition of Pd was conducted in a 0.1 M NaCl solution containing $PdCl_2$ as the precursor with the concentration varied over the range 10^{-4} to 10^{-5} M. Surprisingly, the morphology of the Pd electrodes thus obtained was strongly dependent on the precursor concentration as evidenced by SEM investigation. Figure 1 shows the two typical morphologies, Pd nanorods (Pd-NRs) and Pd nanoparticles (Pd-NPs), obtained in 3×10^{-4} M $PdCl_2$ and 10^{-5} M $PdCl_2$, respectively. The deposition times were adjusted to achieve the same coulometric charge and thus the same amount of Pd deposited.

The diameter of the Pd-NP in Figure 1B ranges from 5 to 10 nm, while the Pd-NRs in Figure 1A are rather uniform in shape with a diameter of ∼5 nm and an aspect ratio of ∼8. Upon increasing the precursor concentration from 10^{-5} to 10^{-4} M, one can observe a gradual transition in the morphology from nanoparticles to nanorods (Figure S1).

(105) Norwak, D. E.; Blasini, D. R.; Vodnick, A. M.; Blank, B.; Tate, M. W.; Deyhim, A.; Smilgies, D. M.; Abruña, H. D.; Gruner, S. M.; Baker, S. P. *Rev. Sci. Instrum.* **2006**, *77*, 113301.

(106) Open source software at http://www.camd.dtu.dk/software.aspx.

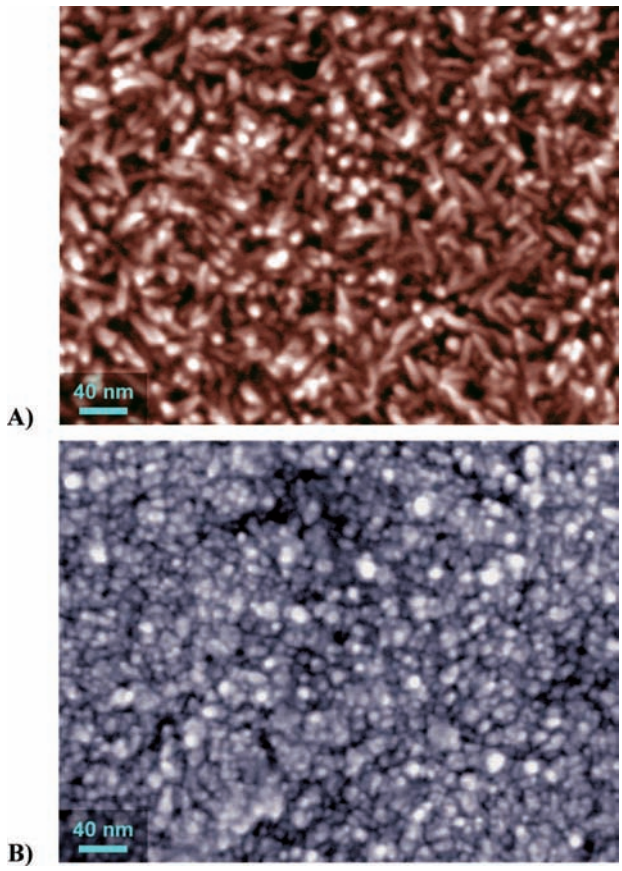

Figure 1. SEM images of two typical morphologies of Pd obtained by adjusting the precursor concentration and deposition time: (A) Pd nanorods (Pd-NRs), 3×10^{-4} M $PdCl_2$, 100 s; (B) Pd nanoparticles (Pd-NPs), 1×10^{-5} M $PdCl_2$, 3000 s.

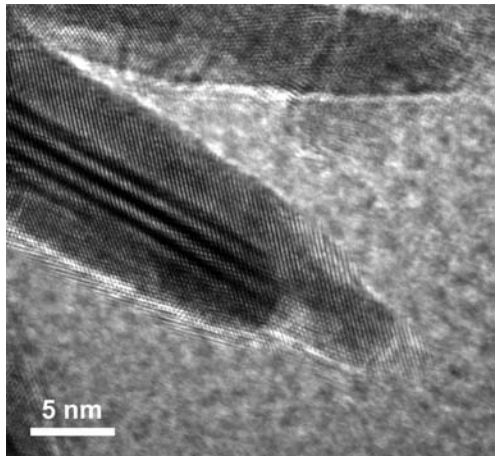

Figure 2. A TEM image of Pd-NR deposited on carbon powder using the same conditions of Figure 1A. Refer to Figure S2 for overviews.

Whereas nanoparticles represent the usual form of synthetic catalysts, nanorods are not generally obtained, especially by a simple electrochemical deposition process, without surfactants. To have a closer look at the Pd-NR crystals, we have deposited Pd-NRs on carbon powders (Figure S2A) so as to be able to peel them off from the electrode and examine them under a TEM (Figure S2B). Figure 2 is a high resolution TEM image of a Pd-NR, in which two or three overlapping single-crystal Pd-NRs with a clear rod shape can be resolved.

In the course of this work, Xia and co-workers[107] reported a chemical synthesis of Pd-NRs using Br^- as the morphology controlling agent, poly(vinyl pyrrolidone) (PVP) as the capping agent, and ethylene glycol (EG) as the reductant. In their approach, Br^- was found to be the best choice, relative to Cl^- and I^-, for obtaining high aspect-ratio nanorods. While the motivation of the present work was not to mimic their approach in an electrochemical fashion, we did try to replace the NaCl electrolyte with KBr. However no Pd deposition occurred under the applied potential, which could be due to a negative shift in the deposition potential caused by the stronger coordinating effect of bromide. We also found that the deposition potential was critical for obtaining Pd-NRs; outside the potential range -0.2 ± 0.1 V (vs Ag/AgCl in 0.1 M NaCl solution), the well-defined rod-shape morphology could not be produced even when using a high concentration of $PdCl_2$.

The mechanism of the electrochemical formation of Pd-NRs in the present work likely shares some similarities to that in Xia's report,[107] including the use of a morphology controlling agent and the control of reduction kinetics. In both cases, a halide, Cl^- or Br^-, was found to be necessary for morphology control. Interestingly, F^- was recently found to be the key in the synthesis of special crystallographic TiO_2.[108] This kind of unusual crystallography is caused, in essence, by selective interactions between the halide and particular facets, which leads to an anisotropic growth of the crystal. We will further discuss this, in detail, on the basis of experimental and computational results in the following sections. In addition to the morphology controlling agent, the reduction kinetics turned out to be another determining factor for obtaining Pd-NRs; a fast reduction rate was found to be crucial for the anisotropic growth of Pd crystals.

Distinct Activities toward ORR. As mentioned in the Introduction, the motivation of the present work was to study the Pd-catalyzed ORR. We found that whereas Pd-NP exhibited "normal" activity as reported for nanosized Pd catalysts obtained from ordinary syntheses, Pd-NRs exhibited, unexpectedly, a much higher activity toward the ORR. Figure 3A presents a comparison of the normalized ORR profiles of Pd-NRs and Pd-NPs with typical data for Pt presented for comparison. To compare the intrinsic activity, the current densities in Figure 3A have been normalized to the geometric surface area (*GSA*) as well as the electrochemical surface area (*ESA*) corresponding to a roughness factor (*RF*), defined as the ratio of *ESA* over *GSA*, of 10.

The procedure for normalizing these ORR profiles involves three steps. First, extracting the kinetic current (I_k) from the measured overall current (I) via the following equation:

$$\frac{1}{I} = \frac{1}{I_L} + \frac{1}{I_k} \tag{1}$$

where I_L is the diffusion limited current which should be normalized to the *GSA* of the electrode to produce the diffusion limited current density (j_L):

$$j_L = \frac{I_L}{GSA} \tag{2}$$

(107) Xiong, Y.; Cai, H.; Wiley, B. J.; Wang, J.; Kim, M. J.; Xia, Y. *J. Am. Chem. Soc.* **2007**, *129*, 3665.
(108) Yang, H. G.; Sun, C. H.; Qiao, S. Z.; Zou, J.; Liu, G.; Smith, S. C.; Cheng, H. M.; Lu, G. Q. *Nature* **2008**, *453*, 638.

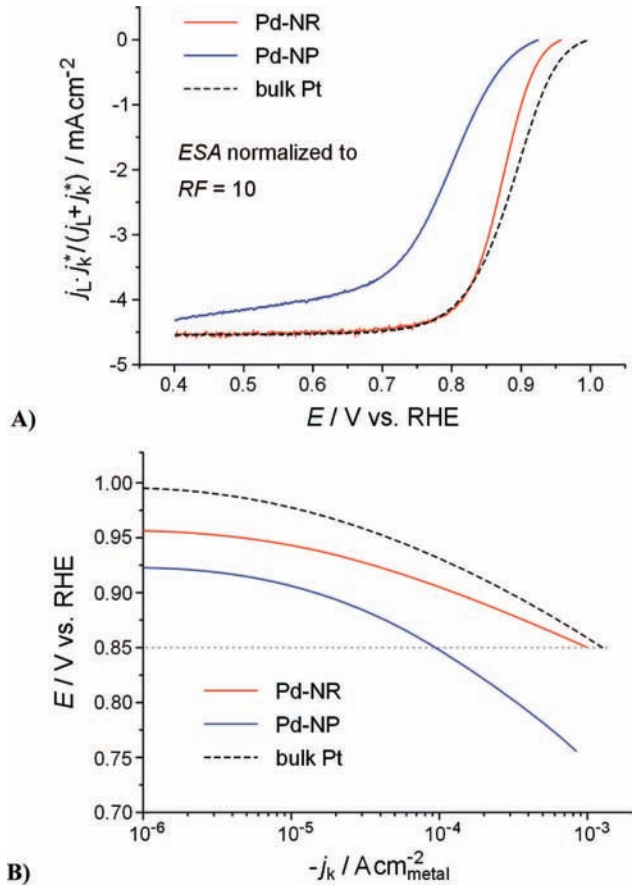

Figure 3. ORR data for Pd-NR, Pd-NP, and bulk Pt, obtained in an O_2 saturated 0.1 M $HClO_4$ solution at a rotation rate of 900 rpm and a scanning rate of 10 mV/s. (A) Normalized ORR profiles. The diffusion limited current (j_L) has been normalized to the geometric surface area (*GSA*), while the kinetic current density (j_k*) has been normalized to an electrochemical surface area (*ESA*) corresponding to a roughness factor (*RF*) of 10. (B) Tafel plots. The kinetic current density (j_k) is normalized to the *ESA* of the corresponding electrode.

Second, normalizing I_k to the *ESA* of the corresponding electrode to produce the kinetic current density (j_k):

$$j_k = \frac{I_k}{ESA} \tag{3}$$

Whereas the *GSA* can be simply measured, being 0.164 cm^2 for all the electrodes; *ESA* requires a detailed process to be described in the next section. Third, reconstructing the normalized overall current density (j*) with an *RF* of 10:

$$\frac{1}{j^*} = \frac{1}{j_L} + \frac{1}{10 \cdot j_k} = \frac{1}{j_L} + \frac{1}{j_k^*} \tag{4}$$

i.e.,

$$j^* = \frac{j_L \cdot j_k \cdot 10}{j_L + 10 \cdot j_k} = \frac{j_L \cdot j_k^*}{j_L + j_k^*} \tag{4a}$$

Plotting j* as a function of the electrode potential (Figure 3A) retains the pristine view of an ORR profile yet with the kinetic component being normalized, enabling a direct comparison in the half-wave potential ($E_{1/2}$). It is evident that, upon switching from Pd-NP to Pd-NR, the $E_{1/2}$ shifts positively by 85 mV and approaches that of Pt.

The Tafel plots of the above data (Figure 3B) emphasize the comparison in j_k, a kinetic parameter representing the surface-specific activity (*SSA*) of an electrocatalyst. Although the j_k of Pd-NRs is still lower than that of Pt at low overpotentials, it increases faster upon polarization. At +0.85 V, a practical operating potential of a PEMFC cathode, the j_k of a Pd-NR approaches that of Pt and is 10-fold higher than that of a Pd-NP.

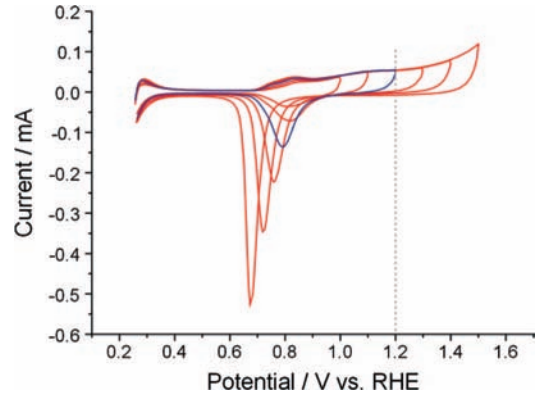

Figure 4. Representative CVs of a Pd electrode in a deaerated 0.1 M $HClO_4$ solution with a scanning rate of 50 mV/s and different upper potential limits. The charge of the cathodic peak in the CV with an upper potential limit of 1.2 V was used for determining *ESA*.

To the best of our knowledge, this is the first observation that, without alloying with foreign metals, pure Pd can be made, through morphology tailoring, to be essentially as active as Pt for the ORR. We deliberately chose the ORR data of bulk Pt, rather than that of nanosized Pt, for comparison because of the well-documented observation that the j_k of nanosized Pt toward the ORR decreases with the particle size and is lower than that of bulk Pt (Figure S3).[109−113] If the comparison was to be made with Pt nanoparticles, which are used in fuel cell applications, the Pd-NR would clearly have superior *SSA*.

Determination of the *ESA* of Pd. In the above analyses, the *ESA* is required to deduce j_k. For Pt, the charge for the underpotential deposition (UPD) of hydrogen is frequently used to calculate the *ESA*. For Pd, unfortunately, the charge of hydrogen UPD cannot be accurately obtained because of the interference of hydrogen absorption in Pd. We tried to employ the UPD of Cu, but the current peaks of Cu UPD are not well-defined in this case (Figure S4), leading to a large uncertainty in integrating the UPD charge.

In the present work, we have employed the reduction charge of surface $Pd(OH)_2$ to determine the *ESA*. As presented in Figure 4, a well-defined cathodic peak can be resolved in the CV of a Pd electrode, but the associated charge is dependent on the upper limit of the potential scan. We chose +1.2 V as the appropriate potential limit because, as indicated in the Pourbaix pH−potential diagram (Figure S5), +1.2 V is the upper limit for the formation of $Pd(OH)_2$ in a solution of pH = 1, and also, as can be clearly seen in Figure 4, above +1.2 V there is the onset of a new anodic process corresponding to the further oxidation of the Pd surface.

(109) Mayrhofer, K. J. J.; Strmcnik, D.; Blizanac, B. B.; Stamenkovic, V.; Arenz, M.; Markovic, N. M. *Electrochim. Acta* **2008**, *53*, 3181.
(110) Yano, H.; Inukai, J.; Uchida, H.; Watanabe, M.; Babu, P. K.; Kobayashi, T.; Chung, J. H.; Oldfield, E.; Wieckowski, A. *Phys. Chem. Chem. Phys.* **2006**, *8*, 4932.
(111) Mayrhofer, K. J. J.; Blizanac, B. B.; Arenz, M.; Stamenkovic, V. R.; Ross, P. N.; Markovic, N. M. *J. Phys. Chem. B* **2005**, *109*, 14433.
(112) Maillard, F.; Martin, M.; Gloaguen, F.; Léger, J.-M. *Electrochim. Acta* **2002**, *47*, 3431.
(113) Kinoshita, K. *J. Electrochem. Soc.* **1990**, *137*, 845.

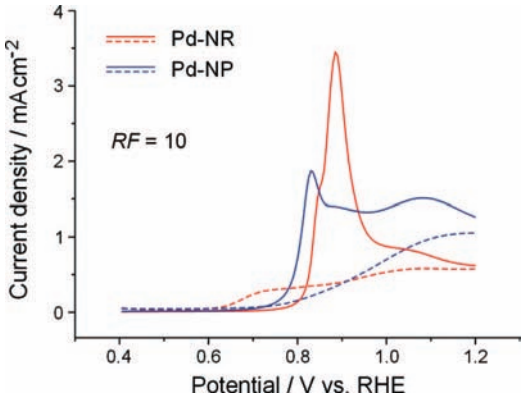

Figure 5. *I*−*V* curves for CO stripping (solid line) and for the bare surfaces (dashed line) on Pd-NR and Pd-NP in a CO-free 0.1 M $HClO_4$ solution at a scanning rate of 50 mV/s. The currents of these curves have been normalized to an *ESA* corresponding to an *RF* of 10.

The charge density for the formation of a fully covered $Pd(OH)_2$ layer was chosen to be 430 $\mu C/cm^2$, which is the minimum of the reported values for typical single-crystal Pd surfaces.[114] The possible error of this charge−surface area conversion might lead to an overestimate of the *ESA* but an underestimation of the value of j_k of Pd. Thus, the above statement about the activity of Pd-NRs toward the ORR being virtually the same as that of (bulk) platinum represents a conservative estimate.

Morphology of Pd-NRs. According to GID measurements, both Pd-NRs and Pd-NPs exhibit the normal fcc pattern of Pd metal (Figure S6), indicating that the superior activity of Pd-NRs toward ORR catalysis is not due to bulk effects such as lattice strain, as observed in Pd alloys,[55] but rather, it can only be ascribed to the morphology of the Pd-NRs themselves.

Because it is difficult to ascertain, in detail, the morphology and chemical characteristics from TEM images, we have also employed the electrochemical CO stripping method, a highly surface-sensitive measurement, to reveal morphological differences between Pd-NRs and Pd-NPs.

Since the CO adsorption strength is sensitive to the nature of the metal substrate (including surface structure), stripping CO from different facets of Pd can yield profiles with characteristic peak potentials and line shapes (Figure S7).[114] As detailed in Figure 5, the CO stripping profiles for Pd-NRs and Pd-NPs are dramatically different. For Pd-NRs, a sharp peak appears around +0.9 V with a shoulder on the low potential side, closely matching the features of CO stripping on Pd(110) (Figure S7B). For Pd-NPs, on the other hand, CO stripping occurs over a rather broad range of potentials; a peak around +0.8 V can be ascribed to Pd(100) facets (Figure S7C), while the broad hump at higher potentials could be due to the Pd(111) facets (Figure S7A) and other disordered structures. The simple and sharp line shape observed for Pd-NRs also indicates that the surface structure of Pd-NRs is relatively homogeneous.

Interestingly, the oxidation curves for the bare surfaces of Pd-NRs and Pd-NPs (dashed lines in Figure 5), albeit relatively featureless, also reflect the difference in the morphology. For Pd-NRs, oxidation of the bare surface occurs at potentials negative to that of CO stripping; whereas that is not the case for Pd-NPs. This seemingly simple feature of Pd-NRs, actually, also matches the unique characteristics of Pd(110) facets (Figure S7B).

(114) Hara, M.; Linke, U.; Wandlowski, Th. *Electrochim. Acta* **2007**, *52*, 5733.

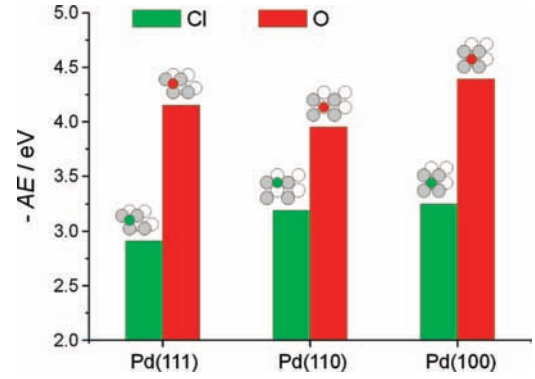

Figure 6. Adsorption energies (*AE*) of Cl and O on Pd(111), Pd(110), and Pd(100), obtained from DFT calculations. Illustrated on the histogram is the preferred adsorption site of Cl (green) or O (red) on the corresponding surface (gray and white indicate the first and the second layer of Pd atoms, respectively).

Figure 5 illustrates the electrochemical fingerprints for the morphology of Pd-NRs and Pd-NPs and provides clear and compelling evidence that the morphology of Pd-NRs is characterized by the exposure of (110) facets, which are usually lacking on the surface of nanoparticles.[9,113,115] We believe that it is such a morphology peculiarity that accounts for Pd-NRs' unusual properties and electrocatalytic activity.

First-Principles Understanding for the Formation and Activity of Pd-NRs. To gain further insights into the morphology−activity relationship of Pd toward the ORR, we have conducted a series of DFT calculations to address the adsorption of different species on different Pd facets. We were particularly interested in the adsorption of Cl and O; the former is related to the morphology control while the latter can serve as a descriptor for the catalytic activity toward the ORR.[31,55] Figure 6 presents the adsorption energy (*AE*) of Cl and O on the three low index facets of Pd. For Cl adsorption, the *AE* sequence is Cl/Pd(100) ≈ Cl/Pd(110) > Cl/Pd(111). Such a difference in the *AE* of Cl on Pd facets could be the thermodynamic factor inducing (being responsible for) the formation of Pd-NRs: the relatively weaker adsorption of Cl on the Pd(111) facets would lead to a preferential growth along the axis perpendicular to {111} facets, leaving {110} and {100} facets to be the side surfaces of nanorods.

For O adsorption on Pd facets, the *AE* sequence turns out to be O/Pd(100) > O/Pd(111) > O/Pd(110). The lowest *AE* of O on Pd(110) is particularly unusual because the surface reactivity of Pd(110) is higher than that of Pd(111) (vide infra), which would, in general, give rise to a stronger adsorption on Pd(110), such as in the case of Cl adsorption. The adsorption of Cl and O on Pd(110) facets also differs in the preferred adsorption site (Figure 6). Whereas Cl adatoms favor the long bridge site, O adatoms prefer to adsorb at the hollow sites. Such a difference in the adsorption site for Cl and O does not occur, however, on Pd(100) or Pd(111) facets.

The exceptionally weak adsorption of O on Pd(110) was not observed on its Pt counterpart. On all low index Pt facets, both Cl and O adsorption follow the same trend (Figure S8); the *AE* sequence for both Cl and O adsorption is Pt(110) > Pt(100) > Pt(111), with a difference in the preferred adsorption sites of Cl and O occurring on Pt(111) rather than on Pt(110) facets.

On plotting all the above-mentioned *AE* values as a function of the *d*-band center (E_d), relative to the Fermi level (E_F), of

(115) Henry, C. R. *Surf. Sci. Rep.* **1998**, *31*, 231.

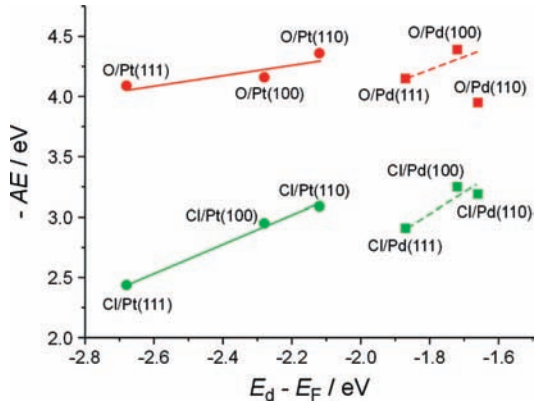

Figure 7. Correlations between *AE* of Cl or O and the *d*-band center ($E_d - E_F$) of Pt or Pd surfaces, showing that O adsorption on Pd(110) deviates significantly from the trend predicted by the *d*-band center theory.

the corresponding facet (Figure 7), one can see how unusually the O/Pd(110) behaves. It is clear that the adsorption trend, of either Cl or O, on Pt facets obeys the *d*-band center theory[116−118] to an acceptable degree; i.e., the *AE* is approximately a linear function of ($E_d - E_F$), and the higher the ($E_d - E_F$) the stronger the adsorption. Such a well-documented principle, however, cannot be applied to the adsorption trend on Pd facets, especially for O adsorption. The *AE* of O/Pd(110) deviates significantly from the would-be linear trend. Although Pd(110) possesses the highest ($E_d - E_F$) among the three basic facets, O/Pd(110) gives unexpectedly the lowest *AE*.

According to our previous studies on the Pd-catalyzed ORR,[55] as well as the reports on the Pt-catalyzed ORR by Nørskov and co-workers,[31] the *AE* of O adsorption can serve as a good descriptor for the catalytic activity of the corresponding surface toward the ORR. For Pd, a general strategy to improve its catalytic activity would be to decrease the *AE* of O adsorption to an appropriate degree.[55] Given that the *AE* of O/Pd(110) is notably lower than that of O/Pd(100) and O/Pd(111), the superior activity of Pd-NRs toward the ORR becomes understandable and most likely arises from the morphology peculiarity of exposing Pd(110) facets at the side surface.

Conclusions

The morphology−activity relationship for practical catalysts is a topic of fundamental and technological significance but has hitherto not been well studied or understood. In this work, we report a strong morphology dependence of the catalytic activity of Pd toward the ORR. Upon changing the morphology of Pd catalysts from nanoparticles to nanorods, the surface-specific activity increases markedly by 10-fold and becomes comparable to that of Pt under fuel cell operating potentials.

The structural peculiarity of Pd-NRs has been shown, through its electrochemical fingerprint on CO stripping, to be the exposure of Pd(110) facets. Furthermore, the adsorption of O on Pd(110) is found, on the basis of DFT calculations, to be exceptionally weak, which is thought to be the intrinsic reason for the superior activity of Pd-NRs toward ORR.

We anticipate the present findings to deepen the understanding of Pd catalysis and guide the rational design of Pd catalysts for the ORR. Follow-up studies on the stability of Pd-NRs and the morphology of Pd alloys are underway in our laboratories.

Acknowledgment. This work was financially supported under the National Hi-Tech R&D Program of China (2007AA05Z142), the Natural Science Foundation of China (20773096, 20433060), and the Program for New Century Excellent Talents in Universities of China (NCET-04-0688). We also acknowledge support by a Department of Energy Grant DE-FG02-03ER46072 and support of the National Science Foundation through the Cornell Center for Material Research Shared Experimental Facilities.

Supporting Information Available: Complete ref 1, supplemental figures, and additional discussions. This material is available free of charge via the Internet at http://pubs.acs.org/.

JA8063765

(116) Hammer, B. *Top. Catal.* **2006**, *37*, 3.
(117) Greeley, J.; Nørskov, J. K.; Mavrikakis, M. *Annu. Rev. Phys. Chem.* **2002**, *53*, 319.
(118) Mavrikakis, M.; Hammer, B.; Nørskov, J. K. *Phys. Rev. Lett.* **1998**, *81*, 2819.